Dense Astrophysical Plasmas

H. M. VAN HORN

Degenerate bodies composed primarily of dense hydrogen and helium plasmas range from giant planets to the so far hypothetical brown dwarfs. More massive objects begin their lives as nondegenerate stars and may end as white dwarfs, composed primarily of carbon and oxygen, or as neutron stars, with solid crusts of iron or heavier elements and cores of neutron matter. The physical properties of dense plasmas that are necessary to construct theoretical models of such degenerate stars include the equation of state, transport properties, and nuclear reaction rates.

In a degenerate plasma, electrons are packed together with the maximum density allowed by quantum mechanics for a given pressure. The packing is so tight that the Pauli exclusion principle, rather than Coulomb repulsion, keeps the electrons apart. These plasmas can occur in the densest astrophysical bodies, such as the interiors of degenerate stars. Degenerate plasmas can be present in objects with masses ranging from approximately $10^{-3}\ M_\odot$, about the mass of Jupiter, up to $0.08\ M_\odot$; such bodies include the giant planets and the so far hypothetical brown dwarfs (*1*). (Here $M_\odot = 1.989 \times 10^{33}$ g is the mass of our sun, the most convenient unit for measuring stellar masses.) These low-mass objects consist primarily of H and He; they never become hot enough to ignite H-burning thermonuclear reactions in their interiors. In contrast, bodies with masses greater than about $0.08\ M_\odot$ are true stars. They are self-luminous, being powered by thermonuclear burning. Stars that are less massive than about 0.7 to $1.0\ M_\odot$, however, burn so slowly that they never leave this main sequence (H-burning) stage of evolution during the entire lifetime of the galaxy (10×10^9 to 20×10^9 years).

Stars with initial masses greater than about $1.0\ M_\odot$ finish H burning while their interiors are nondegenerate. They subsequently undergo core contraction and ignite He-burning thermonuclear reactions when the central temperature and density become sufficiently high. These later stages of stellar evolution are much faster than the initial H-burning phase. Stars in these evolutionary stages also lose mass effectively: Those with initial masses ranging from about 1.0 to about 6 to $8\ M_\odot$ lose enough to end their active, nuclear-burning lifetimes as white dwarfs, typically with masses of about $0.6\ M_\odot$. White dwarf stars (*2*) are bodies supported by the pressure of the degenerate electrons in their interiors. The maximum mass possible for a white dwarf is the Chandrasekhar limiting mass, which has the value $M_{Ch} \approx 1.4\ M_\odot$ for bodies composed of He or heavier elements.

Stars with initial masses greater than about $8\ M_\odot$ cannot lose enough mass during their entire lifetimes to become white dwarfs. In such a star the core continues to contract, passing through stages of ever increasing density and temperature and undergoing further thermonuclear fusion reactions that produce increasingly heavy nuclei. Ultimately, these reactions convert the core to Fe, which has the greatest binding energy per nucleon of any atomic nucleus. Subsequent reactions, therefore, cannot liberate additional energy. The mass of the Fe core continues to grow as matter is processed through the outlying nuclear-burning shells, and when it exceeds approximately $1.4\ M_\odot$ the pressure supplied by the degenerate electrons is no longer sufficient to prevent the star from collapsing under its own gravity. In the ensuing catastrophic collapse, the Fe core is compressed to nuclear densities (about 2×10^{14} g cm^{-3}) in a time scale of seconds. The gravitational energy released in this collapse causes the bulk of the star to explode in a gigantic supernova outburst. Precisely this kind of explosion occurred a few years ago in the star Sanduleak −69 202, which became SN 1987A (*3*). If the stellar remnant of such an explosion has a mass less than about 2 to $3\ M_\odot$, the object is a neutron star (*2*), that is to say a body supported by the pressure of degenerate neutrons. The collapsed cores of the largest stars are too massive to form stable neutron stars, and they are believed to become black holes, objects so dense that even light cannot escape.

In studying these advanced phases of stellar evolution (*4*), it is necessary to know the properties of matter at much higher densities ρ and temperatures T than are generally achievable in terrestrial laboratories. This requires theoretical calculations of (i) pressure $P(\rho,T)$ and entropy $S(\rho,T)$, collectively termed the equation of state; (ii) energy transport properties, such as the radiative opacity and thermal conductivity; and (iii) the nuclear energy production rate $\epsilon(\rho,T)$ and neutrino energy loss rate $\epsilon_\nu(\rho,T)$. From investigations of these properties, it is now known, for instance, that dense plasmas in the cores of white dwarfs and the surfaces of neutron stars freeze solid at sufficiently low temperatures. It is also known that nuclear reactions can occur even at zero temperature if the density is large enough that the quantum mechanical zero-point energy becomes important. From such studies, it has been learned that ionization of hydrogen at low temperature and high pressure may occur via a first-order phase transition. The following sections briefly describe these and other properties of dense plasmas (*5*).

The Equation of State of Dense Matter

For any macroscopic system in thermodynamic equilibrium, P and S can be obtained from the exact relations (*6*)

$$P = -\left.\frac{\partial F}{\partial V}\right|_{T,\{N_Z\}} \qquad S = -\left.\frac{\partial F}{\partial T}\right|_{V,\{N_Z\}} \qquad (1)$$

Here $F(T,V,\{N_Z\})$ is the Helmholtz free energy of the system, which contains the macroscopic numbers N_Z of particles of various species Z in the macroscopic volume V at temperature T. It is often useful to think of this as representing, for example, the properties of

The author is a professor in the Department of Physics and Astronomy, University of Rochester, Rochester, NY 14627.

a cubic centimeter of matter with the values of T and ρ prevailing at some point in a star. Such a small volume contains a macroscopic number of particles, but its dimensions are so much smaller than the scale lengths over which significant variations of the physical quantities occur in stars that it can be well approximated as being in thermodynamic equilibrium.

In a fully ionized plasma at high density, the electrons are strongly degenerate. Their properties depend almost exclusively on ρ and very little on T. This is easily seen for a neutral plasma with a single species of ions of charge Z. If the electron density is $N_e/V = ZN_Z/V \equiv Zn_Z \equiv Z/(4\pi a^3/3)$, then, on average, there are Z electrons confined to a sphere of radius a. From the Pauli exclusion principle, two or more electrons cannot occupy the same quantum state. Thus electrons confined to a volume of dimension a must have different momenta extending up to the Fermi momentum $p_F \sim \hbar/(a/Z^{1/3})$, where $\hbar$ is Planck's constant over 2π. A particle with momentum p_F has a corresponding kinetic energy called the Fermi energy, ϵ_f. For nonrelativistic electrons, where $p_F << m_e c$, we have $\epsilon_f = p_F^2/2m_e$ (m_e is the electron mass and c is the speed of light).

For high enough densities, where $\epsilon_f > kT$, the electrons in the plasma are said to be degenerate (here k is Boltzmann's constant). Because ions are much more massive than electrons, their characteristic energies and their contribution to the plasma energy and pressure are much smaller than those of the electrons. Thus the ions remain nondegenerate to much higher densities than the electrons.

Such dense plasmas are unusual in that the pressure is dominated by the electrons and the thermal properties are dominated by the ions. The mechanical structure of a degenerate star thus is almost completely independent of temperature. The condition of hydrostatic equilibrium then yields a unique radius for each stellar mass and composition, independent of the temperature. Because degenerate stars are initially formed by evolution from a less dense state, and because contraction to higher densities is accompanied by heating, degenerate stars are all born hot. Because stars become degenerate when they have exhausted their nuclear energy resources, and because a degenerate star cannot contract (and heat) further, the evolution of a degenerate star is simply a more or less slow cooling.

The physical conditions in degenerate stellar matter can be illustrated as follows. Consider the cooling of the hot, outer Fe surface layers of a neutron star shortly after it is born. A phase diagram of Fe appropriate for this situation is shown in Fig. 1. Initially the temperature is very high ($T \sim 10^9$ to 10^{10} K), and the thermal energy $kT \geqslant m_e c^2$ is sufficient for spontaneous creation of e^+e^- pairs. In this regime, the plasma emits neutrinos copiously (see below), and because neutrinos escape almost as fast as they are created the neutron star cools rapidly (7). Also, at such high temperatures the plasma is nondegenerate, and the pressure P exerted by thermal radiation exceeds that due to the electrons and ions (to the right of the curve marked $P_{rad} = P_{gas}$ in Fig. 1). Coincidentally, at about this same location Coulomb interactions among the electrons and ions are no longer small compared to kT for an Fe plasma. It has become customary to use the dimensionless parameter $\Gamma \equiv (Ze)^2/akT$ to measure the relative importance of these effects, and for densities above the line marked $\Gamma = 1$ Coulomb effects are important.

When the plasma density is high enough that $\epsilon_f > kT$, the plasma becomes degenerate. For still greater densities, ϵ_f increases more rapidly than the Coulomb energy. Thus interactions with the ions becomes less important for the electrons, and the electron density becomes increasingly uniform. In the extreme, highly degenerate regime, the plasma is well approximated as a noninteracting, uniform-density electron gas in which the ions are embedded. The ions closely resemble the idealized one-component plasma (OCP), a hypothetical system consisting of point, classical (that is, nonquantal) charges in a uniform, neutralizing background. This has become one of the important standard models in statistical physics since its introduction in 1966 (5, 8, 9). Interestingly, in the past several years it has even become possible to perform some experimental tests of the OCP with two-dimensional layers of electrons on liquid He (10) or in GaAs/GaAlAs samples (11) or with three-dimensional arrays of Be ions (12) or electrons (13) in Penning traps. Crystallization of the plasma seems to have been detected in several of these experiments.

At densities large enough (or temperatures low enough) that $\Gamma > 178$, the ion subcomponent freezes into a rigid structure. Accurate Monte Carlo calculations for the OCP (9) show that gradual freezing produces a body-centered cubic (bcc) crystalline lattice. If cooling is sufficiently rapid, however, as may occur during the initial cooling of a neutron star, a disordered Coulomb solid may be formed rather than a crystal (14). Interior to the point at which $\Gamma = 178$ (that is, at higher densities), the plasma in the Fe surface layers freezes solid, forming the surface crust of the neutron star. It is not yet certain whether the neutron star surface is a bcc Fe crystal or a disordered solid.

When the neutron star has cooled sufficiently, the quantum nature of the ions can no longer be ignored. To the left of the line $\hbar\Omega_p = kT$ in Fig. 1, the plasma must be treated as a quantum fluid. Here $\Omega_p^2 = 4\pi(Ze)^2 n_Z/m_Z$ is the square of the ion plasma frequency for ions of charge Z and mass m_Z, and the quantity $\hbar\Omega_p/k$ plays the role of the Debye temperature Θ for the plasma. As T falls below Θ, the

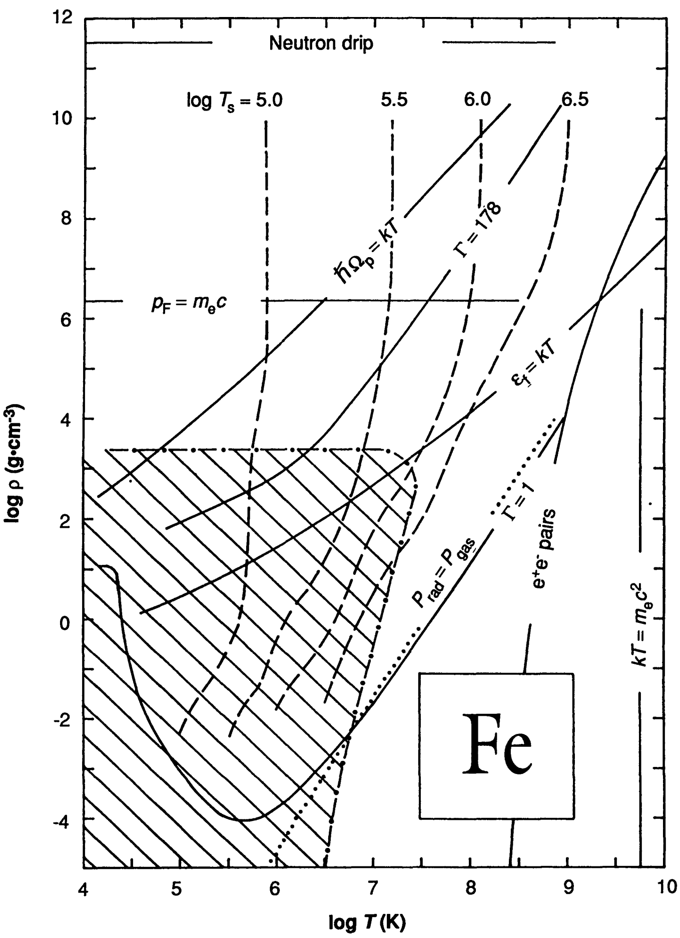

Fig 1. Phase diagram for Fe. The dashed curves represent models for the surface layers of neutron stars with surface temperatures T_s approximately equal to 10^5 K, 3×10^5 K, 10^6 K, and 3×10^6 K. The hatched region in the lower left is the region of incomplete ionization of Fe. See (25) for the equation of state of matter in this regime. [Adapted from (43) with permission]

ion plasma vibrations, which dominate the specific heat of a degenerate plasma, can no longer be thermally excited, and the specific heat declines as $(T/\Theta)^3$ for lower temperatures.

Above the horizontal line marked $p_F = m_e c$ in Fig. 1, the Fermi momentum of the electrons is so high that the electrons become relativistic. At still higher densities, ϵ_f begins to exceed the mass-energy difference between nuclei of different Z, and electron captures begin to occur. This leads to a progressive shift of the equilibrium nuclei to more neutron-enriched species (*15*). When $\rho \gtrsim 4.3 \times 10^{11}$ g cm^{-3} (the horizontal line marked neutron drip), the nuclei have become so neutron enriched that it is energetically favorable for some of the neutrons to appear as free particles, in addition to those that are still present in the neutron-rich nuclei. Finally, for $\rho \gtrsim 2 \times 10^{14}$ g cm^{-3}, which is the density of nuclear matter, the remaining nuclei dissolve. Such extreme densities occur in the cores of neutron stars, where matter consists predominantly of free neutrons with enough free electrons to inhibit neutron decay and enough free protons to make the matter electrically neutral. The strong, short-range nuclear force becomes important here, and the neutron and proton liquids are thought to be superfluids throughout most of the core of a neutron star. Such extreme plasmas are discussed in more detail by Shapiro and Teukolsky (*2*).

Physical conditions similar to those illustrated in Fig. 1 occur in the interiors of cooling white dwarf stars. The deep interiors of these stars are believed to consist primarily of C and O, and the mean densities are less than about 10^6 g cm^{-3} for white dwarfs less massive than about 0.6 $M_\odot$ (the mean mass of a white dwarf). The basic theory of white dwarf cooling is well established (*16*), and the dense plasma effects discussed above for neutron star crusts have been incorporated into detailed calculations (*17*), including the latent heat released upon crystallization and the effects of Debye cooling when T falls below Θ.

Observations (*18*) have shown that the number of white dwarfs declines rapidly for luminosities $L \lesssim 10^{-4.5} L_\odot$, where $L_\odot \approx 4 \times 10^{33}$ erg s^{-1} is the solar luminosity. The most natural interpretation of this is that we are seeing back to the earliest period of star formation in the disk of our galaxy. If so, the cooling age of the white dwarfs to this low luminosity measures the age of the galactic disk. With the best white dwarf models currently available, this is about 10×10^9 years (*19*), which is surprisingly short compared to the ages of the globular cluster stars [about 11×10^9 to 17×10^9 years (*20*)]. The effort to resolve this disagreement has led both to the consideration of alternative models of galaxy formation (*20, 21*) and to explorations of ways to lengthen the white dwarf cooling times. For example, it had been suggested that the dense plasmas in white dwarfs might undergo C/O phase separation, with the denser, O-rich matter sinking to the center (*22*). If it occurred, this process would release substantial gravitational potential energy and prolong the white dwarf cooling. The most recent calculations (*23*), however, have shown that little C/O phase separation actually occurs and that the white dwarf ages are lengthened by no more than about 0.5×10^9 years. Phase separation of heavier elements, such as Ne, from the C/O plasma may also occur, perhaps delaying the cooling by as much as 2×10^9 years (*24*).

As a final example of equation of state calculations, consider the phase diagram of hydrogen (*25, 26*) shown in Fig. 2. The various curves in this figure are similar to those shown in Fig. 1 but do not extend to such high temperatures or densities. The regime shown is that appropriate to the surface layers of white dwarfs, to the interiors of giant planets, and to the interiors of brown dwarf stars, which lie between the white dwarf envelopes and the Jupiter model in Fig. 2. The curve marked $\Gamma = 1$ occurs at much higher densities in this figure than in Fig. 1 because the smaller nuclear charge $Z = 1$ of the protons makes the Coulomb interactions weaker than in the Fe plasma. The line marked $r_s = 1$ shows the density at which the radius $r_s a_0$ of a sphere containing a single electron equals the Bohr radius a. Above this line, where $r_s < 1$, electrons are compressed to dimensions smaller than the ground state of the H atom, and bound atomic states cannot form. As noted above, the OCP freezes solid to the left of the line $\Gamma = 178$. This condition, which applies to a classical plasma, probably does not indicate freezing of the high-density hydrogen plasma, however (*27*); quantum zero-point vibrations of the protons, which become increasingly important above the line marked $\hbar\Omega_p = kT$, delay the formation of the solid phase until much higher Γ values are reached. If solid metallic H^+ can be formed at all, the horizontal dashed line just above $\log \rho = 4$ indicates the best estimate of the density at which the proton lattice undergoes pressure melting (*28*). The curve labeled $\epsilon = 1$ erg g^{-1} s^{-1} shows where thermonuclear and pycnonuclear (density-induced) reactions rapidly consume H (see below).

The shaded region in the lower left portion of Fig. 2 is the regime where hydrogen is incompletely ionized. The upper left boundary of this region is the location of the first-order phase transition (*29*) from liquid to solid molecular H_2. The arrows at the left boundary of the figure, marked H_2 and H, indicate the densities at which the Herzfeld criterion predicts the metallization of molecular and atomic hydrogen, respectively (*26*). The two solid curves separating the neutral H_2 gas-liquid state, the neutral H gas-liquid state, and the fully ionized H^+ plasma correspond to 50% dissociated H_2 and 50% ionized H, respectively. Here $\chi_{H_2} = 2n_{H_2}/(2n_{H_2} + n_H)$ is the degree of dissociation of H_2, and $\chi_H = n_{H^+}/(n_H + n_{H^+})$ is the degree of ionization of atomic H. The narrow, black zone at the upper right of the neutral H_2 region is the so-called plasma phase

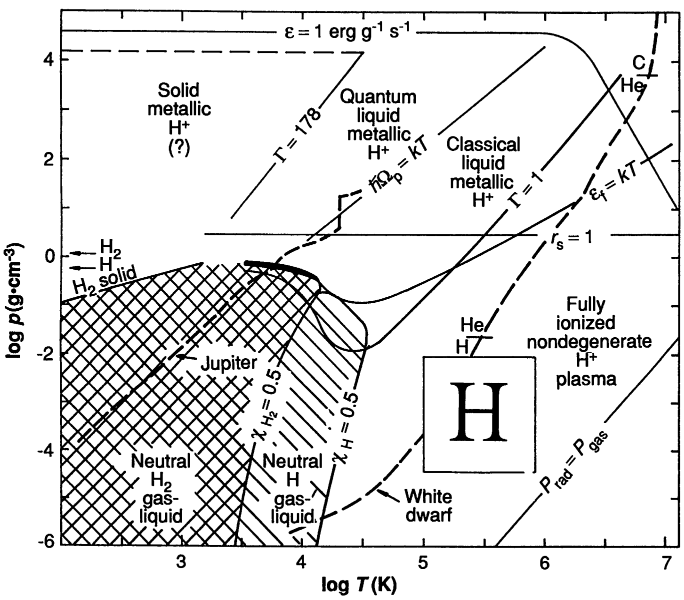

Fig 2. Phase diagram of H. As indicated similarly in Fig. 1, the hatched region in the lower left is the region of incomplete ionization of H. Also shown are ρ-T structure curves of a model for Jupiter that incorporates the PPT (*51*) and of a typical ZZ Ceti pulsating white dwarf model (*52*). The Jupiter model is assumed to be fully convective, and the discontinuous jump in density from $\log \rho = 0.59$ to $\log \rho = 1.27$ marks the boundary of the rocky core. In the white dwarf model shown, the surface layer of H is quite thin, corresponding only to about $10^{-10} M_\odot$, and the maximum density of this region is correspondingly rather low (a bit more than 10^{-2} g cm^{-3}). The underlying He and C layers in this model are shown to indicate the approximate locations of the nondegenerate envelope and the nearly isothermal core. In white dwarfs with thicker H envelopes, as occur, for example, in novae, the H layer extends all the way in, past the degeneracy boundary, to the region where thermonuclear reactions are important. [Adapted from (*26*) and (*53*) with permission]

transition (PPT) (*26, 30*). According to theoretical calculations, liquid molecular H_2 undergoes a first-order transition to a highly (pressure-) ionized, dense plasma phase. The region denoting the PPT terminates in a second critical point near $T = 15{,}300$ K and $\rho = 0.347$ g cm^{-3}, corresponding to $P = 0.614$ Mbar (*26*). These theoretical results have not yet been confirmed by experiment. Shock-wave experiments (*31*), which reach the appropriate range of temperatures and pressures, probably offer the best opportunity to test these ideas. One such experiment (*32*) has actually been interpreted as evidence for the PPT, but the experimental errors are large, and more recent measurements (*31*) do not seem to require this interpretation. Diamond anvil–cell devices can also achieve this range of pressures, although at substantially lower temperatures (*33*).

Energy Transport in Dense Matter

In addition to requiring knowledge of the equation of state, studies of the evolution of dense stars require knowledge of the rates at which heat can be transferred from place to place within the star. This can occur by convection, radiation, or conduction. Convective energy transfer dominates throughout the entire structure of a giant planet or a brown dwarf, but it is important only in the thin surface layers of a white dwarf, and it probably does not occur in neutron stars. Where convection does occur in stars, it is so efficient that the internal temperature distribution is nearly adiabatic, except at the surface. The adiabatic temperature gradient depends only on the equation of state and is not discussed further here.

When radiation is the dominant energy transfer mechanism, the efficiency is determined by the transparency of the stellar matter. The relevant physical property of the plasma is an appropriate frequency-averaged absorption cross section per unit mass called the radiative opacity. Calculations of this quantity are extremely difficult. One must first solve the equations of statistical equilibrium to determine the number densities of each energy level of each ionization state of every ion to be included in the calculation. In principle this information is available from equation of state calculations, but usually not in the detail required for opacity calculations. Trace species, although unimportant for equation of state work, may have large absorption cross sections in regions of the spectrum that are important for the opacity. In addition, the statistical equilibrium calculations are complicated in dense plasmas because Coulomb and other interactions among the different species cannot be neglected. Once the abundances are known, it is necessary to compute absorption coefficients for each level to be considered. This is an even more complicated calculation. For some levels of some ions laboratory data may be known, but for most species this is not the case. It is then necessary to solve the Schrödinger equation, at some level of approximation, to obtain wavefunctions from which the transition probabilities and absorption coefficients can be computed.

The complexity of the numerical calculations required to obtain opacities for dense plasmas makes it understandable why such calculations have until quite recently been performed only at large national laboratories. Indeed, the opacities for various mixtures of astrophysical interest that were obtained at Los Alamos (*34*) remain the current standards for calculations of stellar structure and evolution. Within the past decade, however, several new, independent projects have been initiated to compute new radiative opacities that relax some of the approximations in the pioneering Los Alamos work. One such project, at Lawrence Livermore National Laboratory, has recently demonstrated that a class of nonhydrogenic transitions, between levels with the same principal quantum number in complex ions, can significantly increase the opacity in some regions of Cepheid variable stars (*35*). Interestingly, the region affected is just the one where stellar pulsation calculations have for some time been suggesting that a larger opacity has been needed.

Another complication concerns the effects of molecules, which are not included in the Los Alamos opacities generally used for stellar structure calculations. As astrophysicists and planetary scientists have become more interested in objects of lower temperatures, such as giant planets, brown dwarfs, and even low-mass main sequence stars, the absence of opacities that include molecules has become increasingly troublesome. A few efforts have been made to include the effects of molecules and grains in opacity calculations (*36*) and to study some of their effects, for example, in brown dwarf models (*37*), but the need for additional work in this area is enormous. The most recent such calculation (*38*) includes the latest calculations of the absorption bands of the H_2 molecule for a mixture of pure H and He.

The largest effort to obtain new radiative opacities is the Opacity Project, a multinational collaboration of atomic physicists and astrophysicists led by M. J. Seaton at University College London. This effort has now been under way for more than 7 years. To date, it has produced a new occupation probability formalism to deal with the problem posed by levels at high excitation energies; it has also produced a large, new, atomic database (*39*). Over the next several years, this project has the goal of generating a reliable new radiative opacity database for use in future calculations of stellar atmospheres and interiors.

The final energy transport process, which is by far the most important in sufficiently dense plasmas, is conduction by the degenerate electrons. As in terrestrial metals, scattering by the ions in the plasma is strongly suppressed because the electrons are degenerate. This results in a longer electron mean free path, so that energy can be carried efficiently for long distances. This is the reason for the high thermal (and electrical) conductivities of metals, and it also holds for the degenerate plasmas in dense stars, as has been well understood for more than 50 years. The process is so efficient that the degenerate cores of dense stars are almost completely isothermal (*16, 17, 40*).

Tables of the so-called conductive opacity of degenerate matter, computed more than 20 years ago (*41*), have been used in virtually all calculations of white dwarf star models to date. With the discovery of neutron stars in the late 1960s, and with the realization that both thermal and electrical conductivities were needed for plasmas of much higher densities dominated by very massive ions, interest in the conductivities revived. Calculations have now been published extending from the liquid metal regime into the low-temperature solid phase (*42*). These conductivities are now beginning to be used in calculations of the thermal structures of the deep interiors of white dwarfs (*17*) and the surface layers of neutron stars (*43*) and in studies of the ohmic dissipation of magnetic fields in neutron stars (*44*).

Nuclear and Neutrino Rates

In calculations of thermonuclear reaction rates in plasmas, the reacting ions are treated as a classical gas. The reaction cross sections are computed with the assumption that the ions interact through purely repulsive Coulomb forces until separations of a few times 10^{-13} cm are reached, when the strong nuclear force dominates. This approximation is satisfactory for the conditions found in the centers of most H-burning main sequence stars. In high-density plasmas, however, the reacting nuclei are screened by the surrounding electrons. This weakens the mutual repulsion of the positively charged nuclei, allowing them to approach each other more closely during a collision and increasing the reaction rate (*45*). In the extreme case where $\Gamma > 178$ and the plasma freezes solid, each ion is restricted to the vicinity of its own lattice site. It might be imagined that the reaction rate would vanish in this case, but the quantum mechanical zero-point vibrations of the ions make it possible for reactions still to occur even in this situation. The resulting pycnonuclear reactions are independent of the temperature but increase quite rapidly with increasing density (*46*). This is true "cold fusion," but it requires densities orders of magnitude larger than those used in the recent, controversial cold fusion experiments (*47*).

The zero-point vibrations may also cause the lattice to melt at sufficiently high densities (see Fig. 2). Even in this case, the lattice calculation of the pycnonuclear rates may provide reasonable estimates; each ion can be considered to undergo zero-point vibrations in the cage formed by its nearest neighbors. Calculations based on a quantum fluid description of the plasma, which is necessary for this case, have not yet been performed, however.

The increased sophistication of our understanding of the statistical physics of dense matter has been accompanied by a corresponding increase in the accuracy with which the plasma screening corrections can be calculated. The reaction rate in a dense plasma can be written as the rate in vacuum multiplied by an enhancement factor $f = e^{H(0)}$, where $H(0)$ is the screening potential divided by kT and evaluated at zero separation of the reacting ions. This function can be interpreted as the (dimensionless) difference between the free energies of the plasma before and after the reaction occurs (*48*). This function is now known fairly accurately as a function of Γ for plasmas with a single species of ion and for mixtures (*49*). Calculations of f are most important at very high densities. Such conditions occur in the deep interiors of presupernova stars, in the nuclear-burning shells at the surfaces of the accreting neutron stars (which are x-ray burst sources), or in the accreting white dwarfs that become novae.

Just as the generation of energy by nuclear processes is important in degenerate stars, so is the loss of energy accompanying the emission of neutrinos from these dense plasmas. The reason is that neutrinos interact so weakly with matter that they can escape freely even from the deepest interior regions of neutron stars; the mean free path of a neutrino in nuclear matter exceeds the approximately 10-km radius of the neutron star. Neutrino emission can thus be a powerful refrigeration mechanism in white dwarfs and neutron stars.

The efficiencies of the various neutrino emission processes depend on T and ρ, as do the nuclear energy generation processes. For $T \gtrsim 10^9$ K, spontaneous thermal e^+e^- pair production occurs. Because the weak interaction is a four-fermion process, it is possible for some pairs to annihilate, producing a neutrino-antineutrino pair instead of photons: $e^+ + e^- \rightarrow \nu + \bar{\nu}$. This is called the pair process. At somewhat lower temperatures and at low densities ($\rho \lesssim 10^4$ to 10^5 g cm^{-3}), the dominant mechanism is the photoneutrino process: $\gamma + e^- \rightarrow e^- + \nu + \bar{\nu}$. This is analogous to Compton scattering, except that the final state contains a neutrino-antineutrino pair instead of a photon. At high plasma densities, photons are "dressed" by interaction with the plasma. This changes the energy-momentum relation of the propagating electromagnetic waves, and the resulting entity, termed a plasmon (γ_{pl}), can decay spontaneously into a neutrino-antineutrino pair: $\gamma_{pl} \rightarrow \nu + \bar{\nu}$. Plasma neutrino emission dominates in a band of densities and temperatures centered on the relation $\hbar\omega_p = kT$, where $\omega_p^2 = 4\pi n_e e^2/m_e$ is the square of the usual electron plasma frequency. The final major neutrino emission mechanism is the bremsstrahlung neutrino process, in which a photon decays into a neutrino-antineutrino pair in the field of some heavy nucleus A_Z: $\gamma + A_Z \rightarrow A_Z + \nu + \bar{\nu}$. Expressions for the emissivities for each of these processes are given by Kippenhahn and Weigert (*4*) and by Itoh *et al.* (*50*).

Prospects for the Future

Although much has been learned about the properties of dense plasmas, many questions remain, and there is ample opportunity for further research. One important task is to continue extending dense plasma calculations further into regions where the response of the electron background cannot be neglected (*5*). Such calculations are essential for improved treatments of the PPT and for accurate opacity calculations at high densities, to name just two examples. In addition, the effects of the quantum nature of ions, particularly H and He, need to be investigated. Because these regimes constitute the low-density end of the dense plasma regime, they are also closest to direct experimental study. These is real hope that shock-tube (*31*) or perhaps diamond anvil–cell experiments (*33*) may soon elucidate the true nature of the process by which H undergoes pressure ionization. A related question is whether phase separation occurs in fully ionized binary mixtures at high densities, as with Fe from C in white dwarfs or Fe from H in low-mass stars or brown dwarfs. Phase separation of H from He is known to occur in giant planets, but detailed, new calculations of the phase diagram are needed.

Opacities are another vital area in which significant progress can be expected in the near future as a result of the efforts now being concentrated on this work. Molecular opacities need to be investigated, and plasma dispersion effects also need to be studied. As these results are obtained and applied to investigations of degenerate stars, our understanding of the physical properties of their interiors will continue to improve. We shall then be able to use them increasingly to test broader questions, such as those dealing with the formation of stars and planets and the birth of our galaxy.

REFERENCES AND NOTES

1. M. C. Kafatos, R. S. Harrington, S. P. Maran, Eds., *Astrophysics of Brown Dwarfs* (Cambridge Univ. Press, Cambridge, 1986).
2. S. L. Shapiro and S. A. Teukolsky, *Black Holes, White Dwarfs, and Neutron Stars: The Physics of Compact Objects* (Wiley, New York, 1983).
3. W. D. Arnett, J. N. Bahcall, R. P. Kirshner, S. E. Woosley, *Annu. Rev. Astron. Astrophys.* **27**, 629 (1989).
4. For a detailed discussion of stellar evolution, see R. Kippenhahn and A. Weigert, *Stellar Structure and Evolution* (Springer-Verlag, Berlin, 1990).
5. For a detailed discussion of the properties of dense plasmas, see S. Ichimaru, *Rev. Mod. Phys.* **54**, 1017 (1982); S. Ichimaru, Ed., *Strongly Coupled Plasma Physics* (Elsevier Science/Yamada Science Foundation, Osaka, Japan, 1990).
6. L. D. Landau and E. M. Lifshitz, *Statistical Physics* (Addison-Wesley, Reading, MA, 1958), p. 46.
7. K. Nomoto and S. Tsuruta, *Astrophys. J.* **312**, 711 (1987); K. A. Van Riper, *Astrophys. J. Suppl.* **75**, 449 (1991).
8. S. G. Brush, H. L. Sahlin, E. Teller, *J. Chem. Phys.* **45**, 2101 (1966); J. P. Hansen, *Phys. Rev. A* **8**, 3096 (1973).
9. W. L. Slattery, G. D. Doolen, H. E. DeWitt, *Phys. Rev. A* **21**, 2087 (1980); *ibid.* **26**, 2255 (1982); H. L. Helfer, R. L. McCrory, H. M. Van Horn, *J. Stat. Phys.* **37**, 577 (1984); S. Ogata and S. Ichimaru, *Phys. Rev. A* **36**, 5451 (1987); S. Ichimaru and S. Ogata, in *Strongly Coupled Plasma Physics*, S. Ichimaru, Ed. (Elsevier Science/Yamada Science Foundation, Osaka, Japan, 1990), p. 101.
10. H. W. Jiang and A. J. Dahm, *Phys. Rev. Lett.* **62**, 1396 (1989).
11. V. J. Goldman, M. Santos, M. Shayegan, J. E. Cunningham, *ibid.* **65**, 2189 (1990).
12. L. R. Brewer, J. D. Prestage, J. J. Bollinger, D. J. Wineland, in *Strongly Coupled Plasma Physics*, F. J. Rogers and H. E. DeWitt, Eds. (Plenum, New York, 1987), p. 53; J. J. Bollinger, S. L. Gilbert, D. J. Heinzen, W. M. Itano, D. J. Wineland, in *Strongly Coupled Plasma Physics*, S. Ichimaru, Ed. (Elsevier Science/Yamada Science Foundation, Osaka, Japan, 1990), p. 177.
13. T. M. O'Neill, P. G. Hjorth, B. Beck, J. Fajans, J. H. Malmberg, in *Strongly Coupled Plasma Physics*, S. Ichimaru, Ed. (Elsevier Science/Yamada Science Foundation, Osaka, Japan, 1990), p. 313; J. P. Schiffer, *ibid.*, p. 113.
14. S. Ichimaru, H. Iyetomi, S. Mitake, N. Itoh, *Astrophys. J.* **265**, L83 (1983); S. Ogata and S. Ichimaru, *J. Phys. Soc. Jpn.* **58**, 356 (1989).
15. G. Baym, C. Pethick, P. G. Sutherland, *Astrophys. J.* **170**, 299 (1971); J. W. Negele, in *Physics of Dense Matter*, C. J. Hansen, Ed. (Reidel, Dordrecht, The Netherlands, 1974), p. 1.
16. L. Mestel, *Mon. Not. R. Astron. Soc.* **112**, 583 (1952).
17. D. Q. Lamb and H. M. Van Horn, *Astrophys. J.* **200**, 306 (1975); G. Shaviv, in *White Dwarfs and Variable Degenerate Stars*, H. M. Van Horn and V. Weidemann, Eds. (University of Rochester, Rochester, NY, 1979), p. 11; M. A. Wood, thesis, University of Texas, Austin (1990).
18. J. Liebert, C. C. Dahn, D. G. Monet, *Astrophys. J.* **332**, 891 (1988).

19. D. E. Winget *et al., Astrophys. J.* **315**, L77 (1987); I. Iben, Jr., and G. Laughlin, *ibid.* **341**, 312 (1989).
20. R. B. Larson, in *Dynamics and Interactions of Galaxies,* R. Wielen, Ed. (Springer-Verlag, Berlin, 1990), p. 48.
21. ______, *Mon. Not. R. Astron. Soc.* **176**, 31 (1976).
22. D. J. Stevenson, *J. Phys. Coll.* **41**, C2-61 (1980)
23. S. Ichimaru, H. Iyetomi, S. Ogata, *Astrophys. J.* **334**, L17 (1988); J. L. Barrat, J. P. Hansen, R. Mochkovitch, *Astron. Astrophys.* **199**, L15 (1988).
24. J. Isern, R. Mochkovitch, E. Garcia-Berro, M. Hernanz, *Astron. Astrophys.* **241**, L29 (1991).
25. K. S. Holian, Ed., *T-4 Handbook of Material Properties Data Bases* (Publication LA-10160-MS, UC-34, Los Alamos National Laboratory, Los Alamos, NM, 1984); P. C. Souers, *Hydrogen Properties for Fusion Energy* (Univ. of California Press, Berkeley, 1986).
26. D. Saumon, thesis, University of Rochester, Rochester, NY (1990); ______ and G. Chabrier, *Phys. Rev. Lett.* **62**, 2397 (1989).
27. S. Ichimaru, personal communication.
28. D. Ceperly and B. Alder, *Science* **231**, 555 (1986).
29. M. Ross, F. H. Ree, D. A. Young, *J. Chem. Phys.* **79**, 1487 (1983).
30. W.-D. Kraeft, D. Kremp, W. Ebeling, G. Röpke, *Quantum Statistics of Charged Particle Systems* (Plenum, New York, 1986).
31. M. van Thiel *et al., Phys. Earth Planet. Inter.* **9**, 57 (1974); W. J. Nellis, A. C. Mitchell, M. van Thiel, G. J. Devine, R. J. Trainor, *J. Chem. Phys.* **79**, 1480 (1983).
32. F. V. Grigor'ev, S. B. Kormer, O. L. Mikhailova, A. P. Tolochko, V. D. Urlin, *JETP Lett.* **16**, 201 (1972).
33. R. J. Hemley and H. K. Mao, *Phys. Rev. Lett.* **61**, 857 (1988); H. K. Mao and R. J. Hemley, *Science* **244**, 1462 (1989); H. E. Lorenzana, I. F. Silvera, K. A. Goettel, *Phys. Rev. Lett.* **64**, 1939 (1990).
34. A. N. Cox and J. N. Stewart, *Astrophys. J. Suppl.* **11**, 22 (1965); *ibid.* **19**, 243 (1970); *ibid.,* p. 261.
35. C. A. Iglesias, F. J. Rogers, B. G. Wilson, *Astrophys. J.* **322**, L45 (1987); *ibid.* **360**, 221 (1990).
36. D. R. Alexander, *Astrophys. J. Suppl.* **29**, 363 (1975); ______, H. R. Johnson, R. L. Rypma, *Astrophys. J.* **272**, 773 (1983).
37. J. I. Lunine, W. B. Hubbard, A. Burrows, Y.-P. Wang, K. Garlow, *Astrophys. J.* **338**, 314 (1989).
38. P. Lenzuni, D. F. Chernoff, E. E. Salpeter, *ibid.,* in press; A. Borysow and L. Frommhold, *ibid.* **348**, L41 (1990).
39. W. Däppen, D. Mihalas, D. Hummer, B. Mihalas, *ibid.* **332**, 261 (1988); A. K. Pradhan, in *Atomic Processes in Plasmas,* A. Hauer, Ed. (American Institute of Physics, New York, 1988), p. 59.
40. F. D'Antona and I. Mazzitelli, *Annu. Rev. Astron. Astrophys.* **28**, 139 (1990).
41. W. B. Hubbard and M. Lampe, *Astrophys. J. Suppl.* **18**, 297 (1969).
42. E. Flowers and N. Itoh, *Astrophys. J.* **206**, 218 (1976); N. Itoh, S. Mitake, H. Iyetomi, S. Ichimaru, *ibid.* **273**, 774 (1983); D. G. Yakovlev, *Sov. Astron.* **31**, 347 (1987); S. Mitake, S. Ichimaru, N. Itoh, *Astrophys. J.* **277**, 375 (1984); R. Nandkumar and C. J. Pethick, *Mon. Not. R. Astron. Soc.* **209**, 511 (1984); N. Itoh, Y. Kohyama, N. Matsumoto, M. Seki, *Astrophys. J.* **285**, 758 (1984).
43. E. H. Gudmundsson, thesis, University of Copenhagen, Copenhagen, Denmark (1981).
44. Y. Sang and G. Chanmugam, *Astrophys. J.* **323**, L61 (1987); C. E. Wendell, thesis, University of Rochester, Rochester, NY (1990).
45. E. E. Salpeter, *Aust. J. Phys.* **7**, 353 (1954).
46. A. G. W. Cameron, *Astrophys. J.* **130**, 916 (1959); E. E. Salpeter and H. M. Van Horn, *ibid.* **155**, 183 (1969); S. Schramm and S. E. Koonin, *ibid.* **365**, 296 (1990).
47. M. Fleischmann, S. Pons, M. Hawkins, *J. Electroanal. Chem.* **261**, 301 (1989).
48. H. E. DeWitt, H. C. Graboske, M. S. Cooper, *Astrophys. J.* **181**, 439 (1973).
49. A. Alastuey and B. Jancovici, *ibid.* **226**, 1034 (1978); C. Carraro, A. Schäfer, S. E. Koonin, *ibid.* **331**, 565 (1988); S. Ogata, H. Iyetomi, S. Ichimaru, *ibid.,* in press; S. Ichimaru and S. Ogata, *ibid.,* in press.
50. N. Itoh, T. Adachi, M. Nakagawa, Y. Kohyama, H. Munakata, *ibid.* **339**, 354 (1989); erratum, *ibid.* **360**, 741 (1990).
51. D. Saumon, personal communication.
52. D. E. Winget, thesis, University of Rochester, Rochester, NY (1981).
53. H. M. Van Horn, *Mitt. Astron. Gesellschaft.* **67**, 63 (1987).
54. I thank D. Saumon, S. Ichimaru, and H. L. Helfer for their helpful comments on an earlier version of this article. Supported in part by the National Science Foundation under grant AST 88-20322.

Astrophysical Jets

DAVID S. DE YOUNG

Astrophysical jets are linear structures associated with stars and galaxies which span about seven orders of magnitude in size; the largest jets emanating from galaxies are about 100 times the size of our galaxy and are the largest single objects in the universe. Jets associated with stars are composed of ionized gas moving away from the star with velocities of a few hundred kilometers per second. Extragalactic jets are composed of relativistic particles, magnetic field, and probably additional amounts of cooler ionized plasma either originally ejected in the jet or entrained by it out of the surrounding gaseous medium.The initial outflow velocity for extragalactic jets may be relativistic, and average outflow speeds of several thousand kilometers per second are likely. The energy flux carried by extragalactic jets may be in excess of 10^{46} ergs per second, depending upon the nature of the jet. A definition of jet properties, deduced from their interaction with the ambient medium, can place essential constraints on models for the central power source in the parent galaxy or quasi-stellar object where they originate.

ASTROPHYSICAL JETS ARE ELONGATED AND WELL COLLIMATED structures associated with a variety of astronomical objects that range from single stars to entire galaxies. As the name implies, they are believed to be composed of streams of high velocity gas flowing out from the associated astronomical object, although in some of the most important classes of jet no outflow velocity has been directly measured. Ejection of gas from an astronomical object is a common phenomenon; young stars lose a large amount of their mass in this way, and our own sun produces a solar wind that interacts in a significant way with Earth's magnetosphere. However, these flows are largely spherically symmetric, often with imbedded filamentary structure. Astrophysical jets are unlike these in that they are truly jet-like and not merely a feature of some more general outflow phenomenon. One of the unique aspects of astrophysical jets is that they cover an astonishing range in size. The jets associated with young stars are typically 10^{17} cm in length, while the jets associated with some giant galaxies have an overall extent in excess of 10^{24} cm. These latter objects are the largest single continuous structures found in the universe. Thus the jet phenomenon is seen on scales that cover seven orders of magnitude, yet there is evidence that the important physical processes are much the same in all of them.

Astrophysical jets play a key role in our efforts to understand some

The author is at the Kitt Peak National Observatory, National Optical Astronomy Observatories, Tucson, AZ 85726.